

Ion dominated mechanism for coupling laser energy to plasma

Ayushi Vashistha^{1,2,*}, Devshree Mandal^{1,2}, Atul Kumar^{1,2}, Chandrasekhar Shukla³, Amita Das^{4*}

¹ *Institute for Plasma Research, HBNI, Bhat, Gandhinagar - 382428, India*

² *Homi Bhabha National Institute, Mumbai, 400094*

³ *Samspra Aerospace Systems Pvt. Ltd. Bengaluru, 560008 and*

⁴ *Physics Department, Indian Institute of Technology Delhi, Hauz Khas, New Delhi - 110016, India*

The well-known schemes (e.g. Brunel, resonance, JxB heating etc.,) of laser energy absorption in plasma are mediated through the lighter electron species. In this work a fundamentally new mechanism of laser energy absorption directly through the heavier ion species has been proposed. The mechanism relies on the difference between the ExB drifts of electron and ions in the oscillating electric field of the laser to create charge density perturbations in the presence of a strong external magnetic field. Particle - In - Cell (PIC) simulations using OSIRIS are carried out which provide clear support for this new absorption mechanism at work.

I. Introduction:

There are many well-known schemes by which the laser energy can get absorbed in the plasmas [1, 2]. For instance, resonance, Brunel, JxB heating schemes etc. [3–8], all of which rely on the dynamical response of the lighter electron species. Consequently, the dominant transfer of energy from laser occurs in electron species. However, there are many applications (e.g. fast ignition, medical therapy etc.,) where it is desirable to have energetic ions. This has led to efforts seeking efficient mechanisms of ion heating and/or acceleration [9, 10]. In many previous studies, a two step approach has been envisaged for this objective. The laser energy is first absorbed by electrons which then transfer it to the ions depending on electron-ion classical collisional and/or anomalous processes. Since Rutherford's collision cross section decreases with increasing electron energy, this process is inefficient at high energies [11]. Many ideas of anomalous transfer of energy from electron to ion have also been proposed [12–17]. In this work, we propose a novel scheme by which direct transfer of laser energy to ions is possible.

The new mechanism relies on the application of a strong external magnetic field normal to the laser propagation and the polarization direction. The strength of the magnetic field is chosen such that it restricts the motion of electrons but the heavier ion species remain unmagnetized and are free to move in response to the laser electric field. The $\vec{E} \times \vec{B}$ drift velocity in the presence of externally applied magnetic field and the oscillating electric field is given by

$$\Delta \vec{V}_{\vec{E} \times \vec{B}}(t) = \frac{\omega_{cs}^2}{\omega_{cs}^2 - \omega_l^2} \frac{\vec{E}(t) \times \vec{B}}{B^2} \quad (1)$$

as $\omega_{ce} > \omega_l > \omega_{ci}$, therefore the drift velocity of the two species differ significantly [18]. Here, the suffix $s = e, i$ represents the electron and ion species respectively. Thus, ω_{ce} and ω_{ci} stands for the electron and ion cyclotron frequency respectively. Furthermore, ω_l stands

for the laser frequency. The difference in the drift velocities of electron and ions gives rise to a current. Since, the laser electric field and the externally applied magnetic field, both are perpendicular to the propagation direction, this drift is along the laser propagation direction. This current has a spatial variations at the scale of laser wavelength. Divergence of the current being finite leads to the charge density fluctuation given by the continuity equation:

$$\frac{\partial \rho}{\partial t} + \vec{\nabla} \cdot \vec{J} = 0 \quad (2)$$

This would lead to the excitation of electrostatic plasma mode in the system, thereby, the energy of the laser can get transferred to plasma. We now demonstrate through PIC (Particle - In - Cell) simulations using OSIRIS4.0 that this mechanism is indeed operative, thereby providing clinching evidence for an alternative novel mechanism for laser energy absorption in plasmas.

II. Simulation Details:

We use OSIRIS-4.0 framework [19–21] for our Particle - In - Cell (PIC) studies. The schematics in Fig.1 shows the simulation configuration. A 2-D rectangular simulation box with dimensions $L_x = 3000c/\omega_{pe}$ and $L_y = 100c/\omega_{pe}$ has been chosen. The plasma boundary starts from $x = 500c/\omega_{pe}$ onwards. There is vacuum between $x = 0$ to $x = 500c/\omega_{pe}$. The spatial resolution is taken as 10 cells per electron skin depth corresponding to a grid size $\Delta x = 0.1c/\omega_{pe}$ and time step for calculations is taken to be $\Delta t = 0.02\omega_{pe}^{-1}$. There is a sharp plasma-vacuum interface and a laser is incident from left side on the plasma target. We consider a p-polarized, plane short pulse laser of wavelength $\lambda_l = 9.42\mu m$ corresponding to CO_2 laser. The choice of long wavelength laser is simply for the sake of definiteness and is motivated by the fact that it reduces the requirement of the externally applied magnetic field as we would subsequently show. The mechanism, however, is independent of the

laser wavelength. The normally incident laser is propagating along \hat{x} , centered at $x = 250c/\omega_{pe}$ and has a pulse length ranging from $x = 0$ to $500c/\omega_{pe}$. The number density of the plasma is taken to be $n_0 = 3 \times 10^{20} \text{ cm}^{-3}$ for which the electron plasma frequency is equal to 10^{15} Hz . We have followed the dynamics of both electrons and ion species. The simulations are, however, carried out at a reduced mass ratio of 25 *i.e.* ions are taken to be 25 times heavier than electrons ($m_i = 25m_e$, where m_i and m_e denotes the rest mass of the ion and electron species). This mass ratio has been chosen to reduce the computational time. (The computational resources being meagre at our disposal.) We use normalized units henceforth, unless otherwise stated explicitly. The time is normalized by the inverse of electron plasma frequency corresponding to the chosen plasma density of n_0 . The laser frequency $\omega_l = 0.2\omega_{pe}$. The length is normalized by electron skin depth c/ω_{pe} and the magnetic field by $m_e c \omega_{pe} / e$. The external magnetic field has been chosen in such a way that $\omega_{ce} > \omega_l > \omega_{ci}$. To satisfy this condition the value of magnetic field is chosen to be $B_0 = 2.5$. For this field the electrons gyrate at a frequency $2.5\omega_{pe}$. The number of particles per cell are taken to be 4. Boundary condition along y-axis is considered to be periodic so that we can consider plane infinite laser along y-axis whereas along x-axis, we have chosen absorbing boundary conditions.

The simulation geometry is specifically chosen to avoid the possibility of any well known absorption schemes to be operative. The laser frequency being 0.2 is much smaller than the electron plasma frequency (unity here). The laser is incident normal to the sharp plasma interface. This ensures the absence of resonance and vacuum heating schemes. In addition the role of $\vec{J} \times \vec{B}$ electron heating is made negligible by choosing the laser intensity to lie in the non-relativistic domain of $a_0 = eE/m_e\omega_l c < 1$. Thus the peak intensity of laser in simulation is taken to be $I = 5 \times 10^{15} \text{ W/cm}^2$ with a rise and fall time of $204.6217\omega_{pe}^{-1}$ each.

III. Results:

In Fig 2 we show the lineout of magnetic field of the laser, as well as that generated in the plasma medium at various times for two distinct case (A) and (B) of simulation. The external magnetic field B_0 is chosen to be 0 and 2.5 for Case(A) and (B) respectively. In the figures we denote case (A) by dashed lines and Case (B) by solid lines. It can be observed that in case(A) there is no penetration of the laser magnetic field in the plasma. a complete reflection of the pulse occurs, whereas in case (B) in the presence of external magnetic field there is a finite field which penetrates the plasma medium as can be observed from the second($t=350$), third($t=700$), and fourth($t=1000$) subplots of the figure. In the fourth subplot the laser pulse has left the simulation domain but

there exists a remnant magnetic field disturbance in the plasma.

In Fig 3, we show the evolution of field energy (blue dashed and solid lines for case (A) and Case(B) respectively). The y axis on the left defines their scale. The kinetic energy of electrons and ions are shown by green and red plots respectively. Here the right y axis defines their scale and again dash and solid line represent plots for case (A) and (B) respectively. It is clear from this figure that the initial energy is entirely in the electromagnetic field of the laser pulse. The first dip in the field energy appears when the laser pulse interacts with the plasma. Subsequently, the field energy remains constant (around $t = 380$ to $t = 470\omega_{pe}^{-1}$) and there is another fall from $t = 470\omega_{pe}^{-1}$ onwards. This second fall in the field energy corresponds to the period when the laser pulse leaves the simulation box after reflection. It is interesting to note that for case(A) ultimately the field energy is negligible and only electron kinetic energy is finite. For case(B) on the other hand ultimately the field energy as well as the kinetic energy of both the species are finite. It is interesting to note that electron energy is much smaller in this case as expected. However, the ion energy increases steadily and it is higher than the electron energy. It is clear that as the laser interacts with the plasma in case (B), it excites certain disturbances in the plasma. We also observe that the electrostatic component of the electric field E_x has a significantly higher amplitude (Fig 4(a)) in case(B) as compared to Case(A). The fft shown in Fig 4(b) clearly illustrates that the frequency of the electrostatic disturbances in case(A) correspond to electron plasma oscillations of $\omega = 1$, whereas in Case(B) the frequency seems to have shifted towards lower side indicating the presence of ion dominated mode. The existence of electrostatic field suggests the presence of space charge fluctuations in the system. This can be evidenced from Fig 5 where the ion and electron density profiles of the plasma at two different times (when the laser pulse just hits the plasma surface at around $t = 350\omega_{pe}^{-1}$ and when it has left started leaving the simulation box at $t = 700\omega_{pe}^{-1}$, has been shown in Fig 5). It can be observed from the figure that for case (A) the plasma surface is merely pushed inwards, but both ions and electrons density profiles are identical, thereby maintaining charge neutrality everywhere. However, for case (B) the profiles of the two species are different (resulting in space charge creation) and show oscillations in space. The origin of this space charge field can be understood from the difference in the $\vec{E} \times \vec{B}$ drift velocity of electrons and ions in the presence of a static magnetic field and an oscillating electric field [18].

The preferential transfer of laser energy to ions in the presence of external magnetic field can also be gleaned from the momentum distribution of ions for the two cases at $t = 350$ and $t = 700\omega_{pe}^{-1}$ shown in Fig 6 when the laser is interacting with plasma and has left the simu-

lation domain respectively. It is clearly evident that in the presence of externally applied magnetic field there are significantly larger number of ions which have higher energies.

IV. Conclusion:

In conclusion we would like to re - iterate that the results of the previous section clearly demonstrate that the laser energy gets preferentially coupled to ions in the presence of external magnetic field. The space charge fluctuations created by the difference in the $\vec{E} \times \vec{B}$ velocity of the two species in the presence of the oscillating electric and static external magnetic field appears responsible for the excitation of the electrostatic mode in the plasma medium.

While we have primarily focused here in the illustration of a fundamentally new concept, it should be realised that in recent years there has been a rapid progress in the creation of high magnetic fields in the laboratory. Magnetic field of the order of 1.2 kilo Tesla has already been produced in laboratory [22, 23]. One expects that in near future this limit will increase. We feel that it is only a matter of time when we will witness magnetic field exceeding a value of 14 kilo Tesla at which the mechanism presented in this manuscript can be experimentally verified in laboratory with a long wavelength CO_2 lasers which have now already been made to operate in the pulsed high intensity mode [24–27]

From the arguments given above it is clear the proposed mechanism is giving a dominant role to ions in the absorption of laser energy into plasma. This two dimensional simulation study of normally incident non-relativistic intensity laser is intentionally ideal to isolate this mechanism from other existing mechanisms like JXB, brunel mechanism, resonance absorption etc. This mechanism can be coupled appropriately with the existing absorption mechanisms for electron species to cater energy into ions.

Acknowledgment:

The authors would like to acknowledge the OSIRIS Consortium, consisting of UCLA and IST(Lisbon, Portugal) for providing access to the OSIRIS4.0 framework. Work supported by NSF ACI-1339893. The authors would also like to thank Dr. Ratan Kumar Bera from Institute

For Plasma Research for spending his invaluable time in discussions and giving some very fruitful ideas.

-
- * Electronic address: ayushivashistha@gmail.com, amitadas3@yahoo.co
- [1] P. K. Kaw and J. M. Dawson, “Laser-induced anomalous heating of a plasma,” *The Physics of Fluids*, vol. 12, no. 12, pp. 2586–2591, 1969.
 - [2] P. K. Kaw, “Nonlinear laserplasma interactions,” *Rev. Mod. Plasma Phys.*, vol. 1, p. 15970.
 - [3] Y. Ping, R. Shepherd, B. F. Lasinski, M. Tabak, H. Chen, H. K. Chung, K. B. Fournier, S. B. Hansen, A. Kemp, D. A. Liedahl, K. Widmann, S. C. Wilks, W. Rozmus, and M. Sherlock, “Absorption of short laser pulses on solid targets in the ultrarelativistic regime,” *Phys. Rev. Lett.*, vol. 100, p. 085004, Feb 2008.
 - [4] F. Brunel, “Not-so-resonant, resonant absorption,” *Phys. Rev. Lett.*, vol. 59, pp. 52–55, Jul 1987.
 - [5] W. L. Kruer and K. Estabrook, “Jb heating by very intense laser light,” *The Physics of Fluids*, vol. 28, no. 1, pp. 430–432, 1985.
 - [6] T. H. Stix, “Radiation and absorption via mode conversion in an inhomogeneous collision-free plasma,” *Physical Review Letters*, vol. 15, no. 23, pp. 878–882, 1965.
 - [7] S. Wilks, W. Kruer, M. Tabak, and A. Langdon, “Absorption of ultra-intense laser pulses,” *Physical review letters*, vol. 69, no. 9, pp. 1383–1386, 1992.
 - [8] J. P. Freidberg, R. W. Mitchell, R. L. Morse, and L. I. Rudinski, “Resonant absorption of laser light by plasma targets,” *Phys. Rev. Lett.*, vol. 28, pp. 795–799, Mar 1972.
 - [9] A. E. Turrell, M. Sherlock, and S. J. Rose, “Ultrafast collisional ion heating by electrostatic shocks,” *Nature Communications*, vol. 6, 2015.
 - [10] A. Kumar, C. Shukla, D. Verma, P. Kaw, and A. Das, “Excitation of KdV magnetosonic solitons in plasma in the presence of an external magnetic field,” *Plasma Phys. Control. Fusion*, vol. 61, 2019.
 - [11] P. Gibbon and A. R. Bell, “Collisionless absorption in sharp-edged plasmas,” *Phys. Rev. Lett.*, vol. 68, pp. 1535–1538, Mar 1992.
 - [12] A. Macchi, M. Borghesi, and M. Passoni, “Ion acceleration by superintense laser-plasma interaction,” *Rev. Mod. Phys.*, vol. 85, pp. 751–793, May 2013.
 - [13] L. Robson, P. Simpson, P. McKenna, K. Ledingham, R. Clarke, T. McCanny, D. Neely, O. Lundh, F. Lindau, C.-G. Wahlström, and M. Zepf, “Scaling of proton acceleration driven by petawatt-laser-plasma interactions,” *Nature Physics*, vol. 3, no. 58, pp. 58–62, 2007.
 - [14] A. Henig, S. Steinke, M. Schnürer, T. Sokollik, R. Hörlein, D. Kiefer, D. Jung, J. Schreiber, B. M. Hegelich, X. Q. Yan, J. Meyer-ter Vehn, T. Tajima, P. V. Nickles, W. Sandner, and D. Habs, “Radiation-pressure acceleration of ion beams driven by circularly polarized laser pulses,” *Phys. Rev. Lett.*, vol. 103, p. 245003, Dec 2009.
 - [15] R. A. Snavely, M. H. Key, S. P. Hatchett, T. E. Cowan, M. Roth, T. W. Phillips, M. A. Stoyer, E. A. Henry, T. C. Sangster, M. S. Singh, S. C. Wilks, A. MacKinnon, A. Offenberger, D. M. Pennington, K. Yasuike, A. B. Langdon, B. F. Lasinski, J. Johnson, M. D. Perry, and E. M. Campbell, “Intense high-energy proton beams from

- petawatt-laser irradiation of solids,” *Phys. Rev. Lett.*, vol. 85, pp. 2945–2948, Oct 2000.
- [16] A. P. L. Robinson, M. Zepf, S. Kar, R. G. Evans, and C. Bellei, “Radiation pressure acceleration of thin foils with circularly polarized laser pulses,” *New Journal of Physics*, vol. 10, p. 013021, jan 2008.
- [17] J. Fuchs, P. Antici, E. D’Humières, E. Lefebvre, M. Borghesi, E. Brambrink, C. A. Cecchetti, M. Kaluza, V. Malka, M. Manclossi, S. Meyroneinc, P. Mora, J. Schreiber, T. Toncian, H. Pépin, and P. Audebert, “Laser-driven proton scaling laws and new paths towards energy increase,” *Nature Physics*, vol. 2, no. 1, pp. 48–54, 2006.
- [18] K. Nishikawa and M. Wakatani, “Plasma physics,” *Springer-Verlag, Berlin*, 2000.
- [19] R. G. Hemker, “Particle-In-Cell Modeling of Plasma-Based Accelerators in Two and Three Dimensions,” *Thesis, University of California, Los Angeles*, 2000.
- [20] R. A. Fonseca, L. O. Silva, F. S. Tsung, V. K. Decyk, W. Lu, C. Ren, W. B. Mori, S. Deng, S. Lee, T. Katsouleas, and J. C. Adam, *OSIRIS: A Three-Dimensional, Fully Relativistic Particle in Cell Code for Modeling Plasma Based Accelerators*, pp. 342–351. Berlin, Heidelberg: Springer Berlin Heidelberg, 2002.
- [21] R. A. Fonseca, S. F. Martins, L. O. Silva, J. W. Tonge, F. S. Tsung, and W. B. Mori, “One-to-one direct modeling of experiments and astrophysical scenarios: pushing the envelope on kinetic plasma simulations,” *Plasma Physics and Controlled Fusion*, vol. 50, no. 12, p. 124034, 2008.
- [22] D. Nakamura, A. Ikeda, H. Sawabe, Y. H. Matsuda, and S. Takeyama, “Record indoor magnetic field of 1200 t generated by electromagnetic flux-compression,” *Review of Scientific Instruments*, vol. 89, no. 9, p. 095106, 2018.
- [23] H. Yoneda, T. Namiki, A. Nishida, R. Kodama, Y. Sakawa, Y. Kuramitsu, T. Morita, K. Nishio, and T. Ide, “Strong compression of a magnetic field with a laser-accelerated foil,” *Phys. Rev. Lett.*, vol. 109, p. 125004, Sep 2012.
- [24] D. Haberberger, S. Tochitsky, and C. Joshi, “Fifteen terawatt picosecond CO₂ laser system,” *Optics Express*, vol. 18, no. 17, p. 17865, 2010.
- [25] S. Tochitsky, F. Fiuza, and C. Joshi, “Prospects and directions of CO₂ laser-driven accelerators,” *AIP Conference Proceedings*, vol. 1777, no. 2016, 2016.
- [26] F. N. Beg, A. R. Bell, A. E. Dangor, C. N. Danson, A. P. Fews, M. E. Glinsky, B. A. Hammel, P. Lee, P. A. Norreys, and M. Tatarakis, “A study of picosecond laser-solid interactions up to 10^{19}W/cm^2 ,” *Physics of Plasmas*, vol. 4, pp. 447–457, feb 1997.
- [27] S. Fujioka, Y. Arikawa, S. Kojima, T. Johzaki, H. Nagatomo, H. Sawada, S. H. Lee, T. Shiroto, N. Ohnishi, A. Morace, X. Vaisseau, S. Sakata, Y. Abe, K. Matsuo, K. F. Farley Law, S. Tosaki, A. Yogo, K. Shigemori, Y. Hironaka, Z. Zhang, A. Sunahara, T. Ozaki, H. Sakagami, K. Mima, Y. Fujimoto, K. Yamanoi, T. Norimatsu, S. Tokita, Y. Nakata, J. Kawanaka, T. Jitsuno, N. Miyanaga, M. Nakai, H. Nishimura, H. Shiraga, K. Kondo, M. Bailly-Grandvaux, C. Bellei, J. J. Santos, and H. Azechi, “Fast ignition realization experiment with high-contrast kilo-joule peta-watt LFEX laser and strong external magnetic field,” *Physics of Plasmas*, vol. 23, no. 5, 2016.

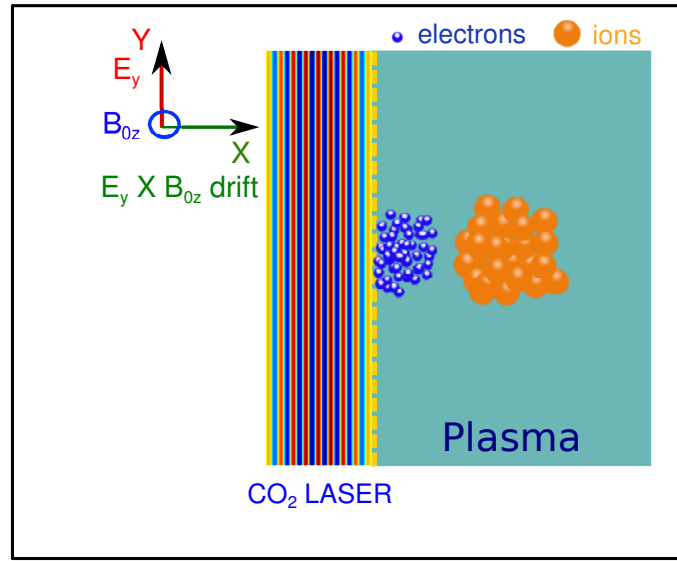


FIG. 1: Schematic (not to scale) showing the direction of electric field of plane infinite laser is along \mathbf{y} and that of magnetic field along with an external magnetic field is along \mathbf{z} and the laser propagation is along \mathbf{x} direction. $\vec{E} \times \vec{B}$ drift is shown to create a charge separation along \mathbf{x}

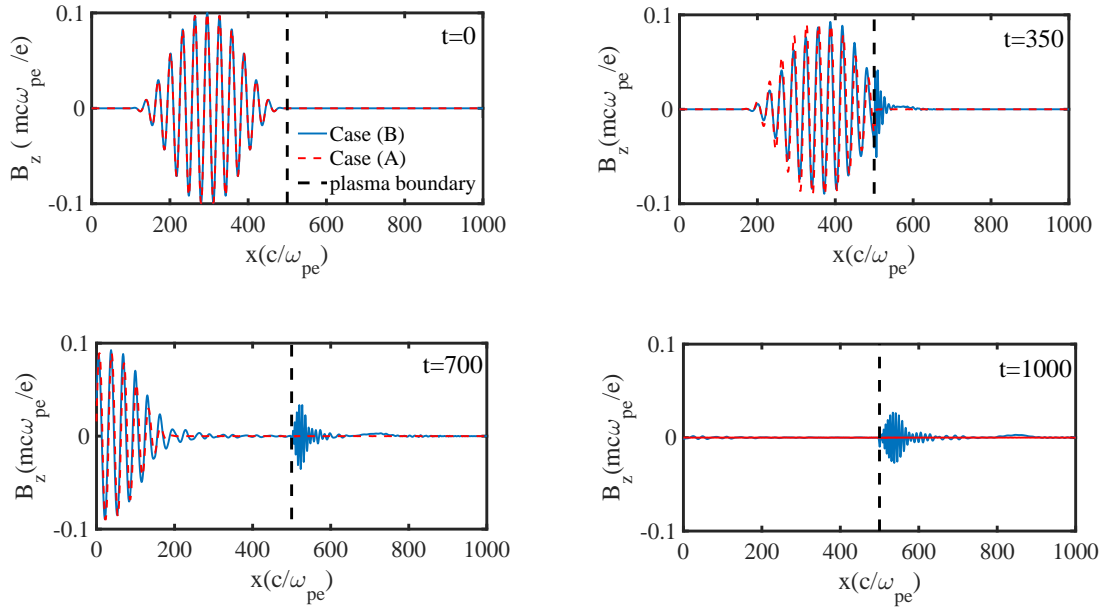


FIG. 2: Time evolution of spatial variation of self generated B_z along \mathbf{x} , averaged over \mathbf{y} , showing that upon interaction with laser there is a finite magnitude of self generated B_z in case(B) which is absent in case (A) .

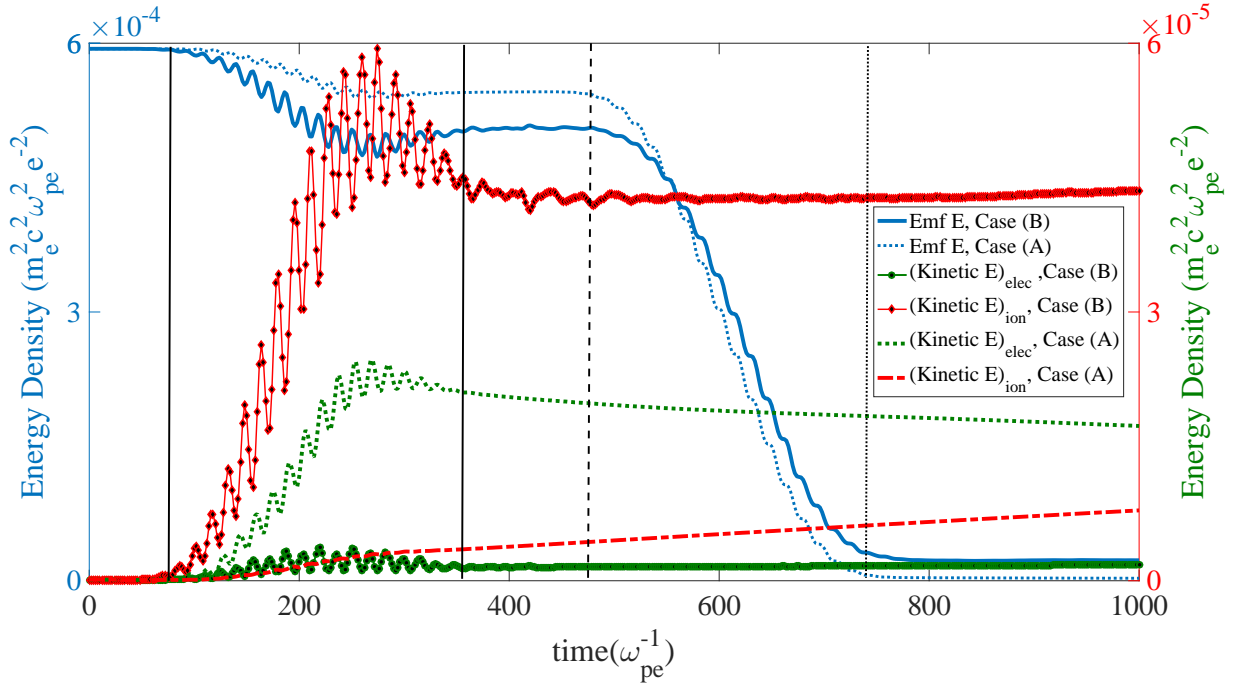


FIG. 3: Time variation of Emf energy of the system and kinetic energies of both the species showing that laser energy is mainly gained by electrons in case(A) and by ions in case (B). The decrease in Emf energy of the system between the two solid lines is due to the interaction of laser with plasma (there is gain in Kinetic energy of electron in case (A) and ions in case(B) at the same time) and between dashed and dotted line is when the laser reflects back from the simulation box. There is also generation of some mode in plasma in case (B) contributing to emf energy of the system even after the laser has been reflected out of the simulation box (beyond dotted line).

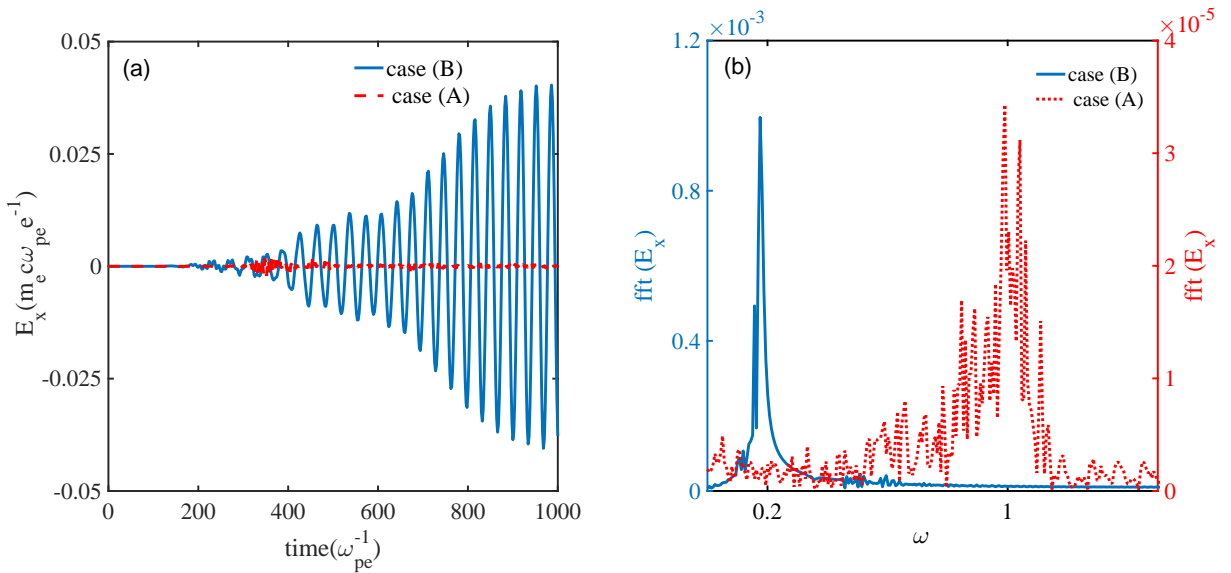


FIG. 4: (a) Time variation of E_x for both the cases at $x=540 c/\omega_{pe}$, averaged over y , depicting generation of electrostatic mode in the bulk plasma in case (A) and case(B). (b) Fast fourier transform of E_x showing peak at electron plasma oscillation for case (A) and at a lower frequency for case (B). The shift in the frequency towards lower end in case (B) indicates towards the presence of an ion dominated mode.

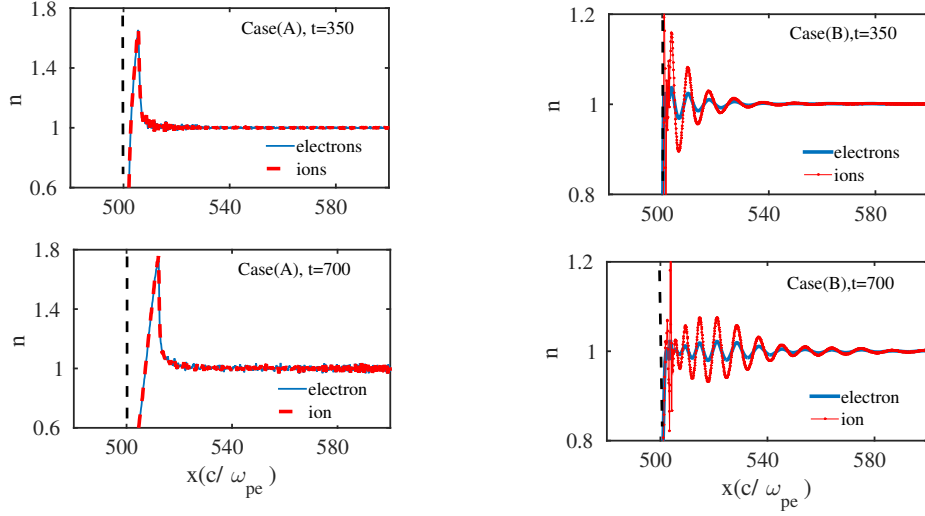


FIG. 5: Spatial variation of density perturbation of both the species along \mathbf{x} , averaged over \mathbf{y} , for case (A) and (B) is depicted showing that density is only perturbed on the laser plasma interface in case (A) whereas in case(B) density perturbations are observed in the bulk plasma as well. Moreover, ion density is perturbed more than electron density showing that laser energy is coupled more into ions.

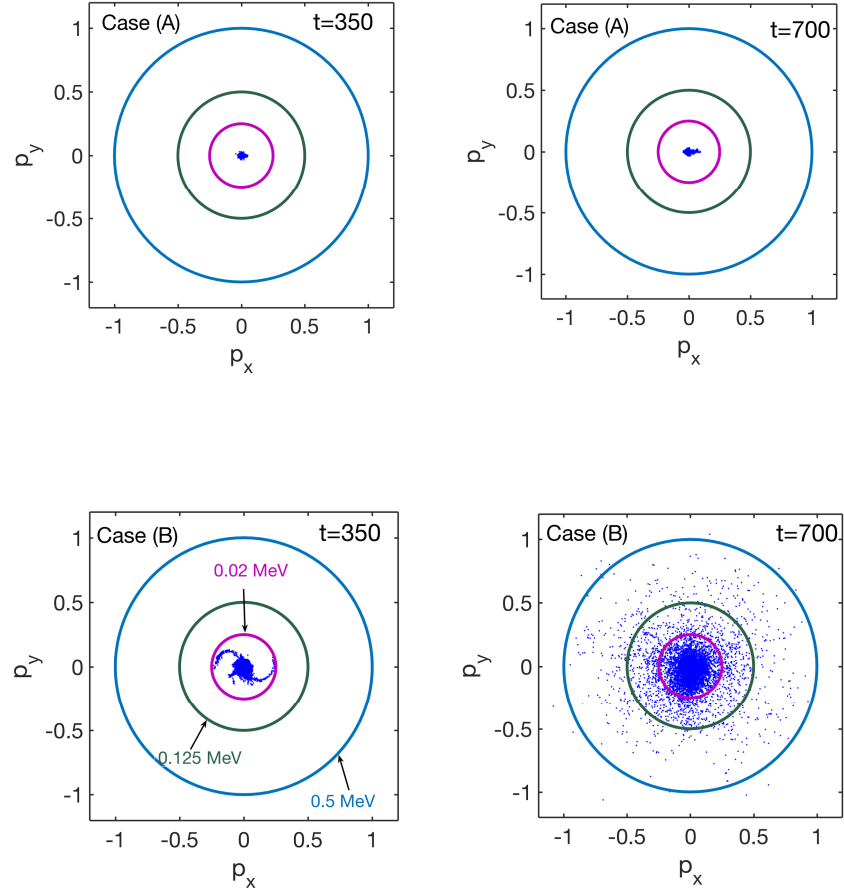


FIG. 6: Temporal evolution of ions distributions in momentum space for case(A) and (B). The figure illustrates that energy is transferred to ions in case(B) and that there is no preferential direction of momenta indicating towards heating of ions.